

See discussions, stats, and author profiles for this publication at: <https://www.researchgate.net/publication/221684107>

Sweet Block Copolymer Nanoparticles: Preparation and Self-Assembly of Fully Oligosaccharide-Based Amphiphile

ARTICLE in BIOMACROMOLECULES · MARCH 2012

Impact Factor: 5.75 · DOI: 10.1021/bm3000138 · Source: PubMed

CITATIONS

25

READS

82

6 AUTHORS, INCLUDING:



[Issei Otsuka](#)

French National Centre for Scientific Research

41 PUBLICATIONS 666 CITATIONS

[SEE PROFILE](#)



[Sebastien Fort](#)

French National Centre for Scientific Research

72 PUBLICATIONS 988 CITATIONS

[SEE PROFILE](#)



[Edson Minatti](#)

Federal University of Santa Catarina

41 PUBLICATIONS 595 CITATIONS

[SEE PROFILE](#)



[Redouane Borsali](#)

French National Centre for Scientific Research

234 PUBLICATIONS 4,363 CITATIONS

[SEE PROFILE](#)

Sweet Block Copolymer Nanoparticles: Preparation and Self-Assembly of Fully Oligosaccharide-Based Amphiphile

Samuel de Medeiros Modolon, Issei Otsuka, Sébastien Fort, Edson Minatti,[†] Redouane Borsali,* and Sami Halila*

Centre de Recherches sur les Macromolécules Végétales, CERMAV-CNRS (Affiliated with Université Joseph Fourier, and member of the Institut de Chimie Moléculaire de Grenoble), BP 53, 38041 Grenoble cedex 9, France

ABSTRACT: The preparation of biocompatible nanocarriers that have potential applications in the cosmetic and health industries is highly desired. The self-assembly of amphiphilic block copolymers displaying biosourced polysaccharides at the surface is one of the most promising approaches. In the continuity of our works related to the preparation of “hybrid” amphiphilic oligosaccharide-based block copolymers, we present here the design of a new generation of self-assembled nanoparticles composed entirely of oligosaccharide-based amphiphilic block co-oligomers (BCO). These systems are defined by a covalent linkage of the two saccharidic blocks through their reducing end units, resulting in a sweet “head-to-head” connection. As an example, we have prepared and studied a BCO in which the hydrophilic part is composed of a free maltoheptaosyl derivative clicked to a hydrophobic part composed of a peracetylated maltoheptaosyl derivative. This amphiphilic BCO self-assembles to form spherical micelles in water with an average diameter of 30 nm. The efficient enzymatic hydrolysis of the maltoheptaose that constitutes the shell of the micelles was followed by light scattering and colorimetric methods.



INTRODUCTION

The sustained interest in amphiphilic block copolymers (BCPs) arises from their ability to self-assemble into a wide variety of morphologies in solution and in thin films, leading to numerous applications such as drug delivery systems,^{1,2} nanoreactors,^{3,4} and nanotemplates.^{5,6} Nanoparticles formed from BCPs are one of the most promising nanocarriers for delivery of hydrophobic or hydrophilic active molecules.⁷ In such applications, some important parameters have to be considered, such as (i) the use of biocompatible and safe biodegradable polymers and (ii) the narrow size distributions of nanoparticles in the size range of 10–100 nm that are ideal for intravenous injection because they are much smaller than the inner diameter ($\geq 4 \mu\text{m}$) of blood capillaries.^{8,9} Thus, many polymeric materials have been reported including poly(L-lactic acid), poly(ϵ -caprolactone), and polypeptides that constitute the hydrophobic inner core, while poly(ethylene oxide), polypeptides, and, more rarely, polysaccharides constitute the hydrophilic outer shell. Most of the combinations between these hydrophobic and hydrophilic polymers have been recently reviewed.¹⁰ Among them, polysaccharides are the most interesting biopolymers because they are abundant, derived from renewable resources, and display various natural biological activities. Typically they are involved in inflammation, cell interactions, pathogen host adhesion, signal transduction development, and a myriad of other processes.¹¹

Very recently, we have carried out work on the preparation and the study of the self-assembly of different “hybrid” block copolymers, based on a well-defined sized oligosaccharide block

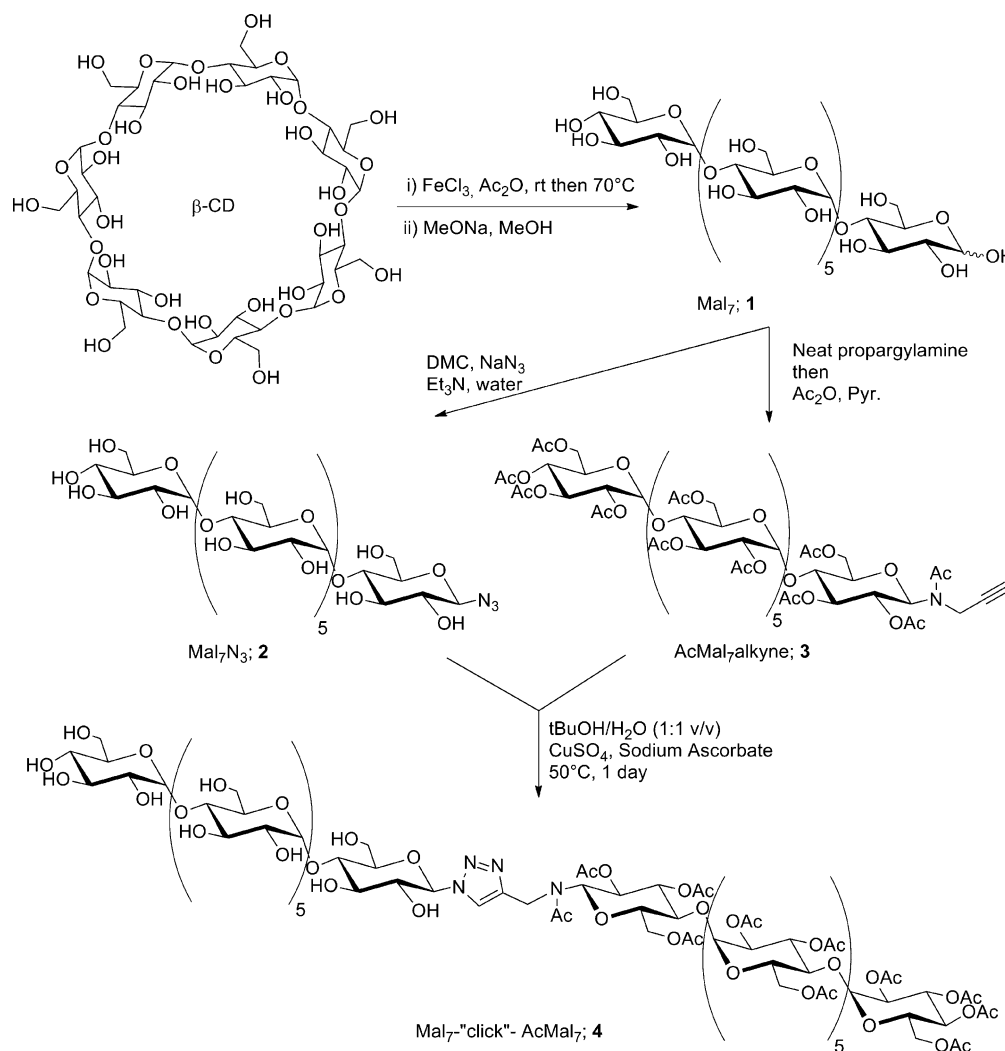
coupled to a functional synthetic polymer block. For instance, we have reported the thermo-responsive PNIPAM-*b*-maltoheptaose block copolymers that self-assembled into narrow vesicular morphologies in water.¹² It was noteworthy that the strong interfacial incompatibility represented by the χ_N (Flory–Huggins constant) between the natural block and the synthetic block enables such self-organization even for low molecular weight oligosaccharide.

This result prompted us to design a new class of linear amphiphilic block co-oligomers (BCO) exclusively constituted of biocompatible and biodegradable saccharidic blocks. As an example, we describe herein the preparation and physicochemical studies of a BCO consisting of a bare maltoheptaose derivative as the hydrophilic block “clicked” to its peracetylated maltoheptaose form as the hydrophobic block. Maltoheptaose 1 is a linear α -(1,4) glucan of seven glucosyl units obtained from the ring-opening of β -cyclodextrin and can be hydrolyzed by starch-degrading enzymes such as glucoamylase or α -amylase. The hydrophobic block was generated by “masking” the hydroxyl groups thanks to ester linkage-mediated hydrophobic protecting groups. Then, the BCO was synthesized by regioselective modification of each block and then linked through Cu(I)-catalyzed azide–alkyne cycloaddition (CuAAC).¹³ The self-assembly behavior in aqueous solution

Received: January 4, 2012

Revised: March 2, 2012

Published: March 7, 2012

Scheme 1. Synthetic Route to Mal₇-“click”-AcMal₇ (4) Block Co-oligomer

was investigated and its sensitivity to *in vitro* enzymatic hydrolysis was carried out.

EXPERIMENTAL SECTION

Materials. β -Cyclodextrin, sodium ascorbate, copper sulfate, and amyloglucosidase (1011S, 67.4 U/mg) were purchased from Sigma-Aldrich and used as received. Water was purified by a Milli-Q water purification system (Billerica, MA, U.S.A.). Maltoheptaose and β -maltoheptaosyl azide (2, Mal₇N₃) were prepared according to the literature.^{14,15}

Instrumentation. Reactions were followed by thin-layer chromatography on silica gel 60F₂₅₄ (E. Merck) by charring with diluted H_2SO_4 . Flash-column chromatography was performed on silica gel 60 (230–400 mesh, E. Merck) or size-exclusion chromatography on a HW40 Toyopearl. ^1H NMR spectra were recorded using 400 MHz Bruker Avance DRX400. Infrared (IR) spectra were recorded using a Perkin-Elmer Spectrum RXI FTIR Spectrometer. MALDI-TOF measurements were performed on a Bruker Daltonics Autoflex apparatus. Fluorescence spectra were recorded on a LS-50B Perkin-Elmer spectrofluorimeter, equipped with a thermostatted cell holder.

Characterization. Mean diameter and the light scattering intensity of the micelles suspension were determined, both by static and dynamic light scattering (SLS and DLS) methods. Measurements were performed using an ALV laser goniometer, which consists of 35 mW HeNe linear polarized laser operating at a wavelength of 632.8 nm, an ALV-5004 multiple τ digital correlator with 125 ns initial sampling time, and a temperature controller. The measurements were recorded

at 90° . The aqueous solutions of Mal₇-“click”-AcMal₇ (4) were filtered directly into the glass cells through a $0.45\ \mu\text{m}$ Millipore Millex PES hydrophilic filter. Data were collected using digital the ALV Correlator Control software. The relaxation time distributions $A(t)$ were obtained using Contin analysis of the acquired autocorrelation functions $C(q,t)$.

Morphological examination of the micelles was conducted using a Kodak SO163 film using a CM200 Philips transmission electron microscope operating at 18 kV. One drop of micelle suspension was placed on a copper mesh covered with nitrocellulose membrane and dried in air before being stained with phosphotungstic sodium solution (1% w/v). An atomic force microscope (AFM PicoPlus; Molecular Imaging) was used to study the surface morphology of the nanoparticles. A 1 drop aliquot of properly diluted micelles was placed on the surface of a clean silicon wafer (ABC, Munich, Germany) and dried under nitrogen flow at room temperature. The AFM observation was performed in tapping mode, with a silicon cantilever of resonant frequency 145–230 kHz.

Synthesis of AcMal₇alkyne (3). The synthesis of N -(2^{1-VII},3^{1-VII},4^{VII},6^{1-VII}-docosa-O-acetyl- β -maltoheptaosyl)-3-acetamido-1-propyne (3, AcMal₇alkyne) was prepared by a method modified from a previously published procedure.¹² Briefly, a suspension of maltoheptaose (10.0 g, 8.67 mmol) in neat propargylamine (11.9 mL, 174 mmol) was stirred vigorously at room temperature for 72 h. The reacting mixture was dissolved in MeOH and then precipitated in CH_2Cl_2 . The solid was filtrated and washed with a mixture of $\text{MeOH}/\text{CH}_2\text{Cl}_2$ (1:3, v/v). The acetylation was carried out by mixing the solid in pyridine with acetic anhydride. The reaction mixture was evaporated

under reduced pressure and the residue was purified by flash chromatography on silica gel (eluent EtOAc–petroleum ether, 70:30 → 90:10) to afford **3** as a white solid, 9.4 g (50%). R_f = 0.4 (7:3 EtOAc–petroleum ether); IR (KBr): ν = 3100–2700 (C–H, sugars), 1644 (C=O, esters, amide) cm^{-1} ; ^1H NMR (400 MHz, CDCl_3): δ = 5.93 and 5.40 (d, J_{1-2} = 9.35 Hz, 1H, rotamers; H-1^{GlcI,Ac}), 5.40 (m, 6H; H-1^{GlcII-VII,Ac}), 5.30–4.80 (m, 44H; H-2, 3, 4, 5, 6^{GlcI-VII,Ac} and NCH_2), 2.32–1.96 ppm (m, 70H; CH_3 (OAc and NAc) and $\text{C}\equiv\text{CH}$); MALDI-TOF: $M + \text{Na}^+$ m/z : 2178.46.

Synthesis of Mal₇–“click”–AcMal₇ (4). The synthesis of 4-[maltoheptaosyl]-1-[N-acetyl-N-(2^{I-VII},3^{I-VII},4^{VII},6^{I-VII}-docosa-O-acetyl- β -maltoheptaosyl)]-5H-[1,2,3]-triazole (**4**, Mal₇–“click”–AcMal₇) was performed by mixing **2** (270 mg, 0.24 mmol) and **3** (500 mg, 0.24 mmol) in water/*t*-BuOH (1:1 v/v) and by adding sodium ascorbate (95 mg, 0.48 mmol) and 0.1 M copper(II) sulfate (2.5 mL, 0.25 mmol). The reaction mixture was stirred at 50 °C for 24 h. The reaction mixture was then evaporated in the presence of silica and the crude solid purified by flash column chromatography (eluent: $\text{CH}_3\text{CN}-\text{H}_2\text{O}$, 90:10 → 80:20) to yield the “clicked” product **4** as a white solid, 500 mg (63%). R_f = 0.42 (7:3 $\text{CH}_3\text{CN}-\text{H}_2\text{O}$); IR (KBr): ν 3600–3100 (O–H, sugars), 3100–2700 (C–H, sugars and alkyl), 1644 (C=O, esters, amide) cm^{-1} ; ^1H NMR (400 MHz, $\text{THF}-d_8/\text{D}_2\text{O}$): δ_{ppm} 8.29 and 8.17 (2x s, 1H rotamers; H-5^{triazole}), 5.85 (m, 1H; H-1^{GlcI,Ac}), 5.60 (m, 6H; H-1^{GlcII-VII,Ac}), 5.00 (m, 6H; H-1^{GlcII-VII}), 4.60 (m, 1H; H-1^{GlcI}), 5.40–3.50 (m, 86H; H-2, 3, 4, 5, 6^{GlcI-VII}, and GlcI-VII,Ac and NCH_2), 2.50–1.80 (m, 69H; CH_3 (OAc and NAc)); HRMS (ESI, m/z): $[M + \text{Na}]^+$ Calcd for $\text{C}_{133}\text{H}_{192}\text{N}_4\text{O}_{93}\text{Na}$, 3356.0315; Found, 3356.0270.

Enzymatic Activity. A total of 3 mg/mL of Mal₇–“click”–AcMal₇ (**4**) was incubated with 6 μL of glucoamylase from *Aspergillus niger* (0.15 mg/mL) in 0.1 M of lithium chloride at 40 °C.

For the bicinchoninic acid (BCA) assay, the reaction tubes were incubated at 40 °C in a reciprocal shaker where 36 μL of sample was regularly taken and diluted up to 500 μL then immediately mixed with BCA reagent (500 μL). The assay is based on the reduction of Cu(II) to Cu(I). The subsequent complexation of Cu(I) and BCA at alkaline pH and elevated temperatures produces an intense purple color. In all experiments, samples of 500 μL were incubated with 500 μL of reagent and heated for 35 min to 75 °C in an oven. The eppendorf tubes were cooled on ice after this and the absorbance was measured at 550 nm using a Bio-Rad 680 microplate reader.

For the follow in SLS and DLS, the biodegradation was conducted at 40 °C inside the cuvette to measure in situ the effective diameter and light scattering intensity with time.

RESULTS AND DISCUSSION

Synthesis and Structural Characterization of Mal₇–“click”–AcMal₇ (4). One of the major problems during the synthesis of amphiphilic molecules is the solubility arising from the different nature of the two blocks. By using proper solvent combinations such as *N,N*-dimethylformamide or hydro-organic medium (acetone, THF, alcohol), the solubility of both blocks can be achieved. The CuAAC reaction is perfectly adapted for such solvent systems and since it is highly chemoselective and compatible with many functional groups such as the hydroxyl groups of polysaccharides, CuAAC is particularly relevant. To address the CuAAC reaction, we introduced the azide and alkyne function at the reducing end of maltoheptaose leading to Mal₇N₃ (**2**) and AcMal₇alkyne (**3**), respectively. This method results in a head-to-head structure, thereby forming the so-called rod–rod block co-oligomers. It is clearly advantageous to directly modify native unprotected sugar because this opens up an avenue for future incorporation of natural polysaccharides without extensive synthetic manipulations.

Maltoheptaose (**1**) denoted by Mal₇ was the key saccharidic block of our synthetic pathway. It was obtained by ring-opening

of β -cyclodextrin using $\text{Ac}_2\text{O}/\text{FeCl}_3$ then deacetylation under Zemplén conditions (catalytic amount of sodium methoxide in methanol) as reported by Liptak et al.¹⁴ Initially the free reducing oligosaccharide Mal₇ (**1**) was chemoselectively functionalized with a propargylamine linker^{12,16,17} and then peracetylated to give AcMal₇alkyne (**3**; Scheme 1). In the second step of our strategic pathway, the maltoheptaosyl azide, Mal₇N₃ (**2**), was prepared according to Shoda’s methodology.¹⁵ The 2-chloro-1,3-dimethylimidazolium chloride (DMC) reagent was demonstrated to be an excellent dehydrating agent for direct activation of the anomeric hydroxyl group of unprotected sugars in aqueous media. The subsequent substitution by azide ions led to the direct synthesis of β -glycosyl azides on various sugars with very good yields. A major concern with this approach is the use of huge quantities of reagent salts and bases, which makes the purification difficult, especially on a large scale. Recently, Vinson et al.¹⁸ have proposed a purification procedure (precipitation and acidic ion-exchange column) that has been ineffective in our hands. Our purification was achieved conveniently by successive steps of acetylation and deacetylation leading to **2** with 77% overall yield.

In the final step of the synthesis, the Mal₇N₃ (**2**) was “clicked” with AcMal₇alkyne (**3**) to produce the block co-oligomer Mal₇–“click”–AcMal₇ (**4**) with a good yield (64%). The later was purified by liquid chromatography on silica gel and then freeze-dried. We are aware that the original form of the CuAAC reaction requires a copper catalyst that is toxic at high micromolar concentrations to cells and organisms. As a result, we have taken care to remove most of the copper salts especially using flash chromatography purification. But we note that one can use other catalytic systems,^{19,20} even Cu-free CuAAC²¹ that could solve the potential problem of Cu toxicity.

The FT-IR spectra showed that the azide group within, Mal₇N₃ (**2**) at 2105 cm^{-1} (Figure 1b), completely disappeared

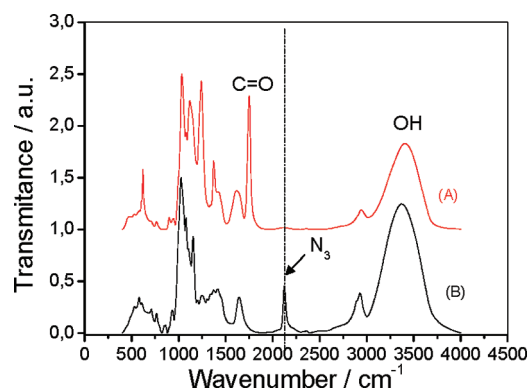


Figure 1. IR spectra of (A) Mal₇N₃ (**2**) and (B) Mal₇–“click”–AcMal₇ (**4**).

in Mal₇–“click”–AcMal₇ (**4**; Figure 1). Moreover, the spectra demonstrated the presence of the acetyl group, as indicated by C=O stretching at 1752 cm^{-1} and the broad band at 3400 cm^{-1} confirmed hydroxyl groups of the free maltoheptaosyl block.

Figure 2a shows the ^1H NMR spectrum of BCO in $\text{THF}-d_8/\text{D}_2\text{O}$ obtained using the “click” reaction. In such a good solvent for both maltoheptaosyl blocks, the proton signals can be clearly seen and the dynamic light scattering (DLS) showed that Mal₇–“click”–AcMal₇ (**4**) essentially exists as unimers whose

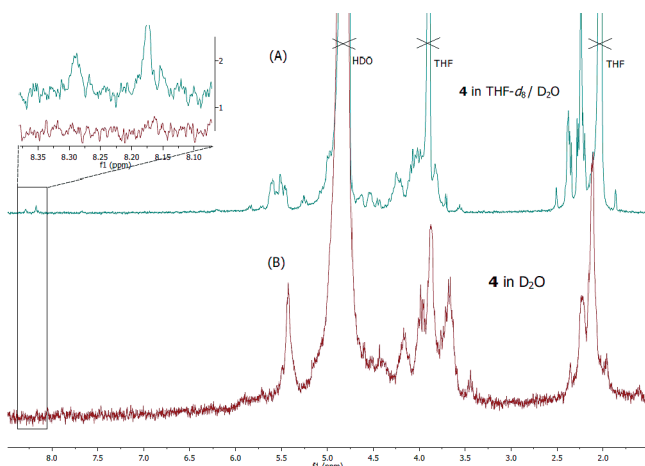


Figure 2. ^1H NMR spectra of Mal₇-“click”-AcMal₇ (**4**) in THF- d_8 /D₂O (1:1 v/v) (above) and D₂O (below).

size are a few nm (results not shown). The BCOs exhibited characteristic peaks of free and acetylated maltoheptaose. The *N*-acetyl group around 2.4 ppm displayed restricted rotations (rotamers), giving rise to a multiplicity of signals in the proton NMR spectra. Moreover, the ^1H NMR spectra showed resonances at $\delta \approx 8.2\text{--}8.3$ ppm, corresponding to the olefinic proton associated with the 1,4-disubstituted 1,2,3-triazole isomer moiety indicating good agreement with assigned structure.

Self-Assembly of Mal₇-“click”-AcMal₇ Co-oligomer in Water. The micelle formation of the diblock co-oligomers in an aqueous condition was first confirmed by comparing the ^1H NMR spectra in THF- d_8 /D₂O (1:1, v/v) and D₂O (Figure 2b). The spectrum recorded in D₂O shows clear signals for the hydrophilic Mal₇ shell while those for the hydrophobic core AcMal₇ and the triazole group are less intense and even disappeared. This indicates that the aggregated AcMal₇ blocks are distributed preferably inside a confined core of the micelles resulting in restricted molecular motion compared to Mal₇ blocks that are located at the outer shell of the micelles in an aqueous phase.

The CMC value for Mal₇-“click”-AcMal₇ (**4**) was determined by the pyrene fluorescent probe method. The measurements of the pyrene fluorescence intensity ratios at I_1/I_3 were measured (Figure 3). This ratio was plotted as a function of BCO concentration to determine the CMC value and the results gave

0.1 mg/mL. The CMC value is within the range reported for low molecular weight nonionic surfactants such as *n*-dodecylmaltoside (0.097 mg/mL) or pentaethyleneglycol-monododecylether (0.027 mg/mL).²² In the field of drug delivery vehicles, this small value is promising and allows us to anticipate the efficient *in vivo* performance and integrity of the micelles even after dilution in bloodstream.

The self-assembly properties of Mal₇-“click”-AcMal₇ (**4**) were investigated in order to highlight their micellar behavior. Nanoparticles were prepared by direct dissolution in deionized water to reach a 0.3 wt % concentration. The size and morphology of Mal₇-“click”-AcMal₇ (**4**) were probed by DLS measurements (Figure 4a) through the angular dependence (q^2 -behavior) of the decay rates of the autocorrelation functions (Figure 4b). The results showed that the BCO self-aggregates in water to form micelles with a hydrodynamic diameter of about 56 nm. The small deviation of the data from the linear fitting in Figure 4b is caused by the very small polydispersity in size of the micelles.

The TEM images of Mal₇-“click”-AcMal₇ (**4**) micelles (Figure 5a) indicate that the micelles had approximately spherical morphology and a smooth surface with minimal aggregation, and the average sizes of the micelles were about 27 ± 4 nm. The investigation by the AFM height image of the micelles was also carried out (Figure 5b). Separate and randomly spherical particles are deposited on the mica surface and appear to be comparatively uniform in size. The height profile was determined along the horizontal line crossing several micelles, as seen in the AFM image (white line). Cross-sectional analysis indicated a micelle diameter of 30–35 nm, in good agreement with those obtained using TEM.

The difference in the diameter of the spherical micelles measured using TEM or AFM (~ 30 nm) comparatively to DLS (~ 56 nm) can be accounted for considering the conditions of observations since in DLS the corona of the micelles is fully solvated while in TEM and AFM the nanoparticles are in dry state. Both the morphologies and the sizes of the micelles did not change within several weeks.

Degradation Behavior of Glucoamylase-Catalyzed Mal₇-“click”-AcMal₇ Micelles. The presence of free maltoheptaose block at the shell of the micelles offers one possibility of enzymatic-mediated drug release. Glucoamylase or amyloglucosidase (EC 3.2.1.3) catalyzes the release of glucose from the nonreducing ends of starch and related maltodextrins²³ such as maltoheptaose (Mal₇). Accordingly, the studies of glucoamylase-catalyzed degradation of Mal₇-“click”-AcMal₇ (**4**)

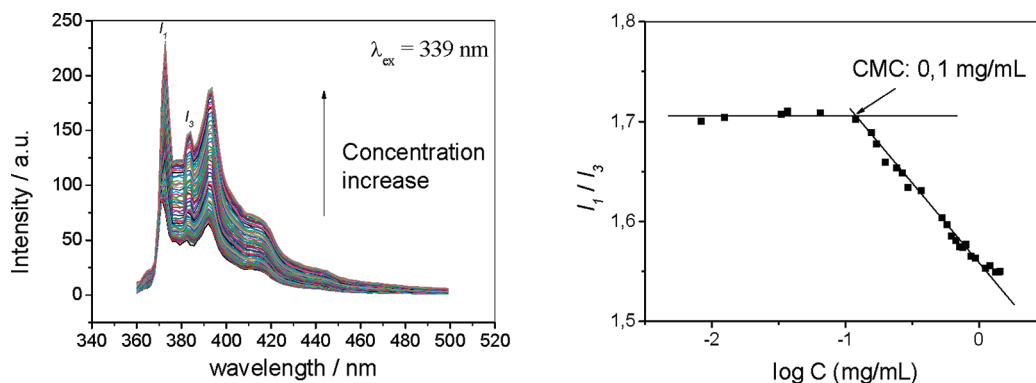


Figure 3. Pyrene fluorescence emission spectra and the corresponding variation in the I_1/I_3 ratio as a function of Mal₇-“click”-AcMal₇ (**4**) concentration ($[\text{pyrene}] = 6.10^{-7}$ mol/L).

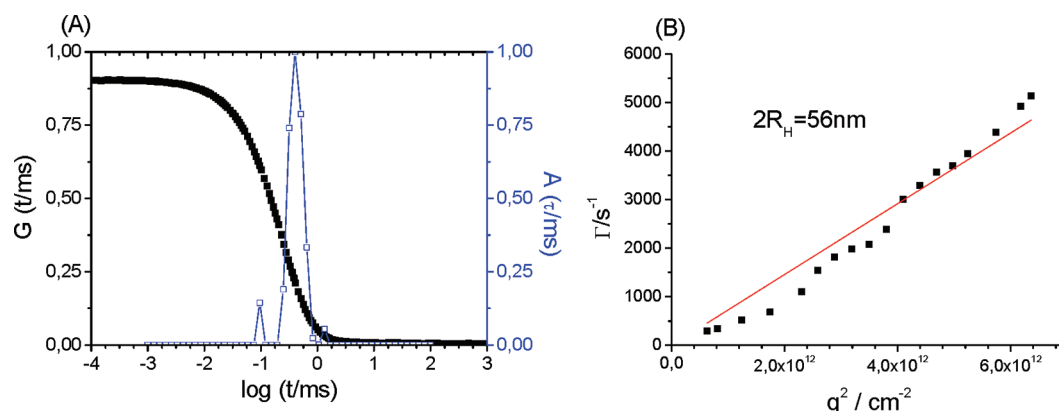


Figure 4. (A) Dynamic light scattering autocorrelation function (circle) and relaxation-time distribution (solid line) of Mal₇-“click”-AcMal₇ (**4**) in water (conditions: Mal₇-“click”-AcMal₇ (**4**) = 3 g·L⁻¹; scattering angle, $\theta = 90^\circ$; temperature, 25 °C). (B) Variation of the relaxation frequency (Γ) vs the square of the wave vector (q^2).

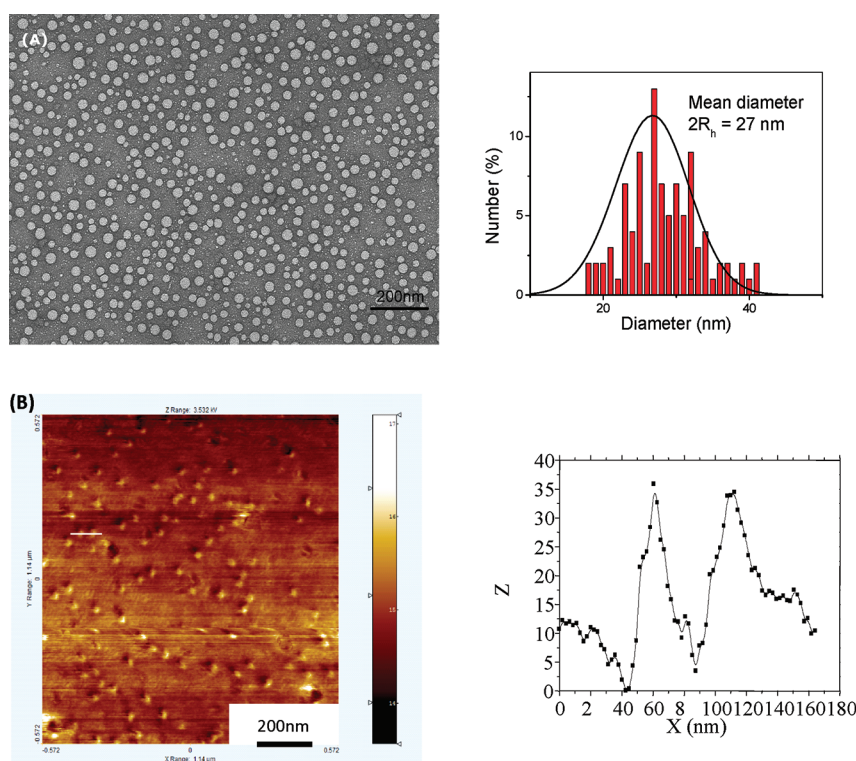


Figure 5. (A) Transmission electron micrograph (bar 200 nm) with size distribution and (B) tapping mode AFM phase images with sectional analysis of Mal₇-“click”-AcMal₇ micelles (**4**; 3 mg/mL).

were done by static and dynamic light scattering (SLS and DLS) measurements and by reducing sugar assays. The change in light scattering intensity and hydrodynamic size of Mal₇-“click”-AcMal₇ micelles related to the action of glucoamylase were used to probe the enzymatic hydrolysis. Figure 6a shows an increase of the relative scattering intensity that levels off after 2 h. At this stage, one visually observes a precipitation in the reaction mixture. In Figure 6b, the time-dependent average hydrodynamic radius of the micelles indirectly shows that there is a change in their molar mass during the biodegradation. It is noteworthy that this behavior is very different from a degradation of the hydrophobic block where the intensity decreases and the micelle size remains unchanged.²⁴ During the enzymatic degradation, the shell, consisting of maltoheptaose (DP 7), is hydrolyzed to smaller maltooligosaccharides (DP <

7), resulting in a decrease of important factors of stability such as the steric repulsion of the shell and the interfacial free energy between the water and AcMal₇ core. These degraded micelles with higher free energy are unstable in the aqueous solution and must reassemble to form larger aggregates to minimize their free energy that ultimately precipitates.

Alternatively, the degradation in the same conditions of Mal₇-“click”-AcMal₇ micelles by glucoamylase was followed by BCA (bicinchoninic acid) method that is colorimetric assay, which measures the concentration of reducing end-groups as shown in Figure 7. The BCA assay has been shown to give a good accuracy with low concentration of glucose and relatively uniform values when applied to oligosaccharides derived from starch, polygalacturonic acid, and chitin, independently of the degree of polymerization.²⁵ Initially, the hydrolysis rate was

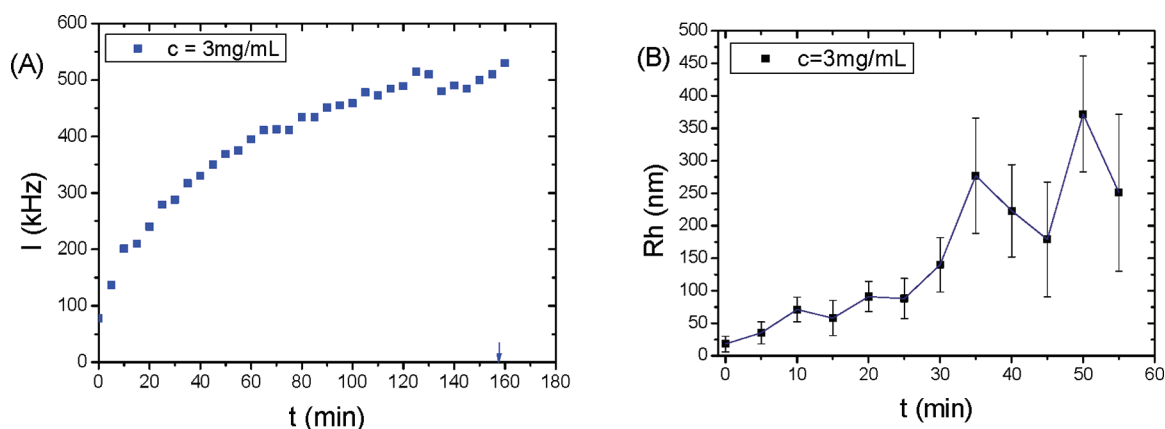


Figure 6. (A) Enzymatic hydrolysis time dependence of relative raw scattering intensity at 90° and (B) of the hydrodynamic radius with 3 mg/mL Mal₇-“click”-AcMal₇ micelles (4). The error bars correspond to the width of the CONTIN size distribution peaks. After 1 h, the correlation function was too bad to obtain a CONTIN fit.

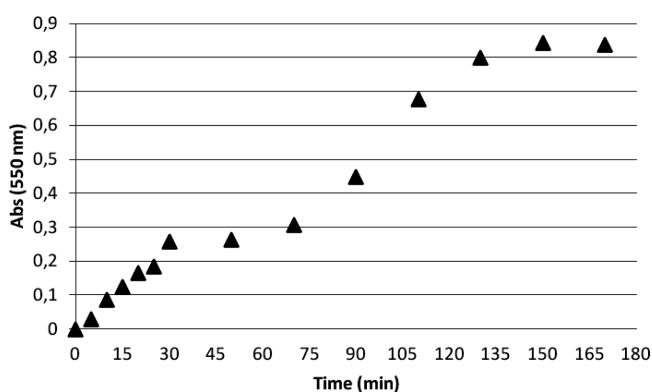


Figure 7. Variation of the absorbance over time when 3 mg/mL of Mal₇-“click”-AcMal₇ micelles (4) were hydrolyzed by glucoamylase. The experiment was carried out in duplicate and the values represent the average.

linear with time but decreased gradually after 30 min. After 75 min, the hydrolysis rate increased again linearly with time and then decreased once more after 120 min. We suggest that in the first instance the Mal₇-containing shell is well-hydrolyzed by the glucoamylase until it becomes less and less accessible. In the second instance, the reassembly might allow a new cycle of hydrolysis up to complete degradation or inaccessible substrates.

CONCLUSION

This work reports for the first time that linear amphiphilic BCOs exclusively constituted of saccharidic blocks can self-assemble in water giving rise to spherical micelles with an average diameter of 30 nm. We have demonstrated, using both light scattering and colorimetric techniques, that the micelles are sensitive to Mal₇-degrading enzymes. Moreover, we have clearly observed a reassembly process of the micelles during the course of the shell hydrolysis. Thanks to the versatility of our approach, the design of a large set of oligosaccharide-based BCOs would be possible by varying, for example, the nature of the protecting groups that is an essential structural parameter for the stability and loading capacity of nanoparticles, the size of the oligosaccharidic blocks, or even the incorporation of biologically relevant carbohydrates. These fully amphiphilic oligosaccharides constitute innovative materials, finding a great interest as biocompatible and biodegradable nanocarriers. For

future studies, we envisage a more detailed unraveling of the mechanism of the micellization process and biodegradation. Work on biological properties such as cytotoxicity, encapsulation, vectorization, and so on will also be carried out.

AUTHOR INFORMATION

Corresponding Author

*Tel.: +33 4 76 03 76 66 (S.H.); +33 4 76 03 76 40 (R.B.). Fax: +33 4 76 54 72 03 (S.H.); +33 4 76 03 76 29 (R.B.). E-mail: sami.halila@cermav.cnrs.fr (S.H.); borsali@cermav.cnrs.fr (R.B.).

Present Address

[†]Laboratory of Polymer and Surfactant Solutions, Federal University of Santa Catarina, Brazil.

Notes

The authors declare no competing financial interest.

ACKNOWLEDGMENTS

Dedicated to Dr. Hugues Driguez on the occasion of his 70th birthday. We are grateful for the help of I. Pignot-Paintrand and A. Durand-Terrasson in the technical assistance with TEM and C. Travelet for dynamic light diffusion experiments. We thank S. Boullanger for MALDI-TOF MS analysis and D. Lesur for ESI-HRMS. We acknowledge the financial support from the CNRS and CAPES-COFECUB (Project 620/08).

REFERENCES

- (1) Miyata, K.; Christie, R. J.; Kataoka, K. *React. Funct. Polym.* **2011**, *71*, 227–234.
- (2) Keddar, U.; Phutane, P.; Shidhaye, S.; Kadam, V. *Nanomedicine* **2010**, *6*, 714–729.
- (3) Renggli, K.; Baumann, P.; Langowska, K.; Onaca, O.; Bruns, N.; Meier, W. *Adv. Funct. Mater.* **2011**, *21*, 1241–1259.
- (4) Che, Q.; Schönherr, H.; Vancso, G. J. *Small* **2009**, *5*, 1436–1445.
- (5) Park, H. J.; Kang, M. G.; Guo, L. J. *ACS Nano* **2009**, *3*, 2601–2608.
- (6) Chao, C.-C.; Wang, T.-C.; Ho, R.-M.; Georgopoulos, P.; Avgeropoulos, A.; Thomas, E. L. *ACS Nano* **2010**, *4*, 2088–2094.
- (7) Oerlemans, C.; Bult, W.; Bos, M.; Storm, G.; Nijssen, J. F. W.; Hennink, W. E. *Pharm. Res.* **2010**, *27*, 2569–2589.
- (8) Gaumet, M.; Vargas, A.; Gurny, R.; Delie, F. *Eur. J. Pharm. Biopharm.* **2008**, *69*, 1–9.
- (9) Malam, Y.; Loizidou, M.; Seifalian, A. M. *Trends Pharmacol. Sci.* **2009**, *30*, 592–599.

- (10) Schatz, C.; Lecommandoux, S. *Macromol. Rapid Commun.* **2010**, *31*, 1664–1684.
- (11) Taylor, M. E.; Drickamer, K. *Introduction to Glycobiology*; Oxford University Press: Oxford, 2003.
- (12) Otsuka, I.; Fuchise, K.; Halila, S.; Fort, S.; Aissou, K.; Pignot-Paintrand, I.; Chen, Y.; Narumi, A.; Kakuchi, T.; Borsali, R. *Langmuir* **2010**, *26*, 2325–2332.
- (13) Kolb, H. C.; Finn, M. G.; Sharpless, K. B. *Angew. Chem., Int. Ed.* **2001**, *40*, 2004–2021.
- (14) Farkas, E.; Janossy, L.; Harangi, J.; Kandra, L.; Liptak, A. *Carbohydr. Res.* **1997**, *303*, 407–415.
- (15) Tanaka, T.; Nagai, H.; Noguchi, M.; Kobayashi, A.; Shoda, S.-I. *Chem. Commun.* **2009**, 3378–3379.
- (16) Halila, S.; Manguian, M.; Fort, S.; Cottaz, S.; Hamaide, T.; Fleury, E.; Driguez, H. *Macromol. Chem. Phys.* **2008**, *209*, 1282–1290.
- (17) Aissou, K.; Otsuka, I.; Rochas, C.; Fort, S.; Halila, S.; Borsali, R. *Langmuir* **2011**, *27*, 4098–4103.
- (18) Vinson, N.; Gou, Y.; Becer, C. R.; Haddleton, D. M.; Gibson, M. I. *Polym. Chem.* **2011**, *2*, 107–113.
- (19) Chan, T. R.; Hilgraf, R.; Sharpless, K. B.; Fokin, V. V. *Org. Lett.* **2004**, *6*, 2853–2855.
- (20) Soriano del Amo, D.; Wang, W.; Jiang, H.; Besanceney, C.; Yan, A. C.; Levy, M.; Liu, Y.; Marlow, F. L.; Wu, P. *J. Am. Chem. Soc.* **2010**, *132*, 16893–16899.
- (21) Jewett, J. C.; Bertozzi, C. R. *Chem. Soc. Rev.* **2010**, *39*, 1272–1279.
- (22) Zhang, R.; Zhang, L.; Somasundaran, P. J. *Colloid Interface Sci.* **2004**, *278*, 453–460.
- (23) Hiromi, K.; Ohnishi, M.; Tanaka, A. *Mol. Cell. Biochem.* **1983**, *51*, 79–95.
- (24) Nie, T.; Zhao, Y.; Xie, Z.; Wu, C. *Macromolecules* **2003**, *36*, 8825–8829.
- (25) Doner, L. W.; Irwin, P. *Anal. Biochem.* **1992**, *202*, 50–53.